

## Threshold and Graded Response Behavior in Human Neutrophils: Effect of Varying G-Protein or Ligand Concentrations<sup>†</sup>

Todd A. Riccobene,<sup>‡</sup> Anna Waller,<sup>‡</sup> Julie F. Hoffman,<sup>‡,§</sup> Jennifer J. Linderman,<sup>‡</sup> and Geneva M. Omann<sup>\*,||</sup>

Department of Chemical Engineering, University of Michigan, Ann Arbor, Michigan 48109, and Departments of Biological Chemistry and Surgery, University of Michigan Medical School and Veteran's Administration Medical Center, Ann Arbor, Michigan 48105

Received December 22, 1997; Revised Manuscript Received April 13, 1998

**ABSTRACT:** Observing the qualitative characteristics of response behavior as key variables in the signal transduction cascade are changed can provide insight into the fundamental roles of these interactions in producing cellular responses. Using flow cytometric assays and pertussis toxin (PT) treatment of human neutrophils, we have shown that actin polymerization stimulated with the chemoattractants *N*-formyl-Met-Leu-Phe, leukotriene B<sub>4</sub>, and interleukin-8 exhibits threshold behavior in terms of G-protein number. Partial PT treatment resulted in both responding and nonresponding populations of cells upon stimulation. As PT treatment was increased, the responding population of cells continued to respond maximally, while the number of cells responding decreased. We also showed that *N*-formyl peptide-stimulated oxidant production exhibits threshold behavior in terms of G-protein number, and the threshold for oxidant production is significantly greater than that for actin polymerization. The threshold behavior observed with PT treatment contrasted with the graded response behavior seen when cells were stimulated with different doses of ligand. For actin polymerization, only one population of cells was observed at submaximal ligand concentrations, and as ligand concentration was decreased the whole population responded submaximally. For oxidant production, as ligand concentration was decreased there were two populations of cells, but the responding cells responded submaximally. A mathematical model incorporating receptor/ligand binding and G-protein activation was developed to account for these differences in response behavior. Our results predict that an early signal transduction event in addition to, and not initiated by G-protein activation, is necessary to account for actin polymerization and oxidant production in neutrophils.

Cellular responses are governed to a large extent by the binding of ligands to cell surface receptors and the signal transduction events that follow. Observing the qualitative characteristics of response behavior as key variables in the signal transduction cascade are changed can provide insight into the fundamental roles of these interactions in producing cellular responses. For example, as the concentration of a signaling molecule is increased in a graded manner, the response may also increase in a graded manner, or the response may increase slowly until a particular concentration is reached and then increase very sharply to a maximum. This latter type of response behavior is often referred to as threshold or all-or-none behavior, and is observed for many types of responses [e.g., actin polymerization in neutrophils (1–3), Ca<sup>2+</sup> elevation in helper T-cells (4), BC<sub>3</sub>H1 cells (5), and bovine smooth muscle cells (6)].

The type of response behavior observed can suggest what type of molecular mechanisms are involved in producing the response. An example of this is given by Huang and Ferrell (7) and Kholodenko et al. (8), who show that threshold behavior can be achieved by having a number of enzymes that follow Michaelis–Menten type kinetics in series. Here we focus on varying the number of G-proteins and ligand/receptor complexes participating in signal transduction in human neutrophils. Using a combination of experimental data and mathematical modeling, we provide insight into the mechanisms involved in producing the observed response behavior.

Neutrophils, or polymorphonuclear leukocytes, are a critical component of the host defense mechanism and inflammatory response. They circulate in the blood until activated by the binding of chemoattractants to specific cell surface receptors. These chemoattractants include *N*-formyl peptides, leukotriene B<sub>4</sub> (LTB<sub>4</sub>),<sup>1</sup> and interleukin-8 (IL-8), each of which has its own receptor. The binding of chemoattractants leads to a complex series of responses including chemotaxis, phagocytosis, oxidant production, and

<sup>†</sup> This work was supported by National Science Foundation Grants BES-9410403 and BES-9713856, the Office of Research and Development, Medical Research Service, Department of Veteran's Affairs, and the Cellular Biotechnology Training Program, NIH Training Grant GM08353.

\* Author to whom correspondence should be directed at Research Service (11R), Veteran's Administration Medical Center, 2215 Fuller Road, Ann Arbor, MI 48105. Phone: (734) 769-7100, ext. 5238. Fax: (734) 761-7693. E-mail: gmomann@umich.edu.

<sup>‡</sup> Department of Chemical Engineering, University of Michigan.

<sup>§</sup> Current address: Johnson & Johnson, Raritan, NJ 08869.

<sup>||</sup> Departments of Biological Chemistry and Surgery, University of Michigan Medical School and Veteran's Administration Medical Center.

<sup>1</sup> Abbreviations: CHO-MLF, *N*-formyl-methionyl-leucyl-phenyl-alanine; LTB<sub>4</sub>, leukotriene B<sub>4</sub>; IL-8, interleukin-8; PT, pertussis toxin; DHR-123, dihydrorhodamine-123; NBD, *N*-(7-nitrobenz-2-oxa-1,3-diazol-4-yl); PHPA, parahydroxyphenylacetic acid; CHO-NLFNTK-fl, *N*-formyl-norleucyl-leucyl-phenylalanyl-norleucyl-tyrosyl-lysine-fluorescein.

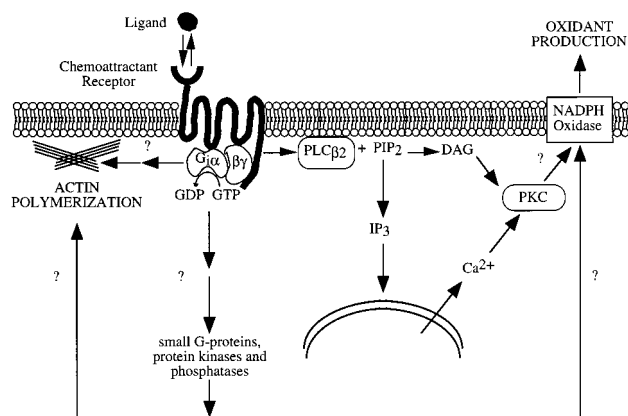


FIGURE 1: Signal transduction pathways leading to actin polymerization and oxidant production. Molecules thought to play a role include the  $\beta_2$  isoform of phospholipase C ( $PLC\beta_2$ ), phosphatidylinositol-4,5 bispophosphate ( $PIP_2$ ), diacylglycerol (DAG), inositol-1,4,5 trisphosphate ( $IP_3$ ), and protein kinase C (PKC). Conversion of receptors to a high-affinity form and interaction of receptors with the cytoskeleton also occur, although the role of these events in signaling is not well-understood.

degranulation. Uncontrolled activation of neutrophil responses can lead to damage of host tissue, and has been implicated in a number of acute and chronic inflammatory diseases (9–11). A quantitative understanding of the signaling mechanisms which lead to these responses is therefore of great importance.

The neutrophil chemoattractant receptors couple to and activate a pool of pertussis toxin (PT) sensitive G-proteins upon binding ligand (12–14). To a large extent, the ensuing responses are mediated by activation of these G-proteins. Figure 1 shows a number of the intracellular events involved in the signal transduction cascade leading to oxidant production and actin polymerization including an increase in intracellular free calcium concentration, and activation of phospholipase C and protein kinase C (12, 15). Many other molecules, such as low molecular weight G-proteins and protein kinases and phosphatases, are known to be involved in oxidant production and actin polymerization, but the details of how they participate in the signal transduction cascade have not yet been clearly defined (14, 16). Because much of the signaling pathway is not known, we chose to focus on the early events in signal transduction up to G-protein activation. Some of these early events, such as the conversion of receptors to a high-affinity form (17–19) and the interaction of receptors with the cytoskeleton (20–22), are G-protein independent but may still influence signaling.

Using flow cytometry in conjunction with PT treatment to examine *N*-formyl-methionyl-leucyl-phenylalanine (CHO-MLF) stimulated actin polymerization and intracellular  $Ca^{2+}$  elevation, Omann et al. (1–3) showed that decreasing the number of functional G-proteins resulted in an increased number of nonresponding cells, while the responding cells continued to respond at a maximal level. Omann et al. (1–3) also showed that the division of cells into responding and nonresponding populations was not caused by differential ADP-ribosylation of G-proteins by PT. These results imply that a threshold number of receptor-coupled G-proteins is required to initiate neutrophil responses. If the number of active G-proteins is reduced below this threshold, the cells

do not respond at all, while cells with greater than the threshold number of G-proteins respond at the maximal level. In contrast, in cells which have not undergone PT treatment, submaximal doses of ligand caused submaximal responses in all cells (graded behavior). It is not known if this threshold behavior is a general phenomena for G-protein coupled chemoattractant receptors and will also be seen with other neutrophil responses.

To test the generality of this threshold phenomenon, we investigated the effect of stimulating neutrophils with the chemoattractants  $LTB_4$  and IL-8 on the actin polymerization response. We also used a flow cytometric assay to show that threshold behavior is seen with CHO-MLF stimulated oxidant production. In addition, to better understand the implications of our experimental results, we have proposed a simple mathematical model of the response behavior which makes the novel prediction that G-protein independent events are important for regulating responses.

## MATERIALS AND METHODS

**Neutrophil Isolation and PT Treatment.** Human neutrophils were partially separated from citrated blood by gelatin sedimentation, and further isolated to >98% purity by counterflow elutriation (23). Following isolation, the cells were resuspended in HSB (5 mM KCl, 147 mM NaCl, 1.9 mM  $KH_2PO_4$ , 0.22 mM  $Na_2HPO_4$ , 5.5 mM glucose, 0.3 mM  $MgSO_4$ , 1 mM  $MgCl_2$ , 10 mM HEPES, pH 7.4) at  $10^8$ /mL. Cells that were to undergo PT treatment were resuspended at  $5 \times 10^7$ /mL in Krebs–Ringer buffer with no  $Ca^{2+}$  and with 5.5 mM glucose, 25 mM HEPES, and 6.3 mg/mL cytochrome C added. PT from List Biologicals (Campbell, CA) was reconstituted to 100  $\mu$ g/mL in sodium phosphate buffer (0.1 M sodium phosphate, 0.5 M NaCl, pH 7.0), giving a final concentration of 0.11 M sodium phosphate and 0.55 M NaCl, and added by dilution to cell suspensions to give the desired final PT concentration. An equivalent amount of PT vehicle (0.11 M sodium phosphate, 0.55 M NaCl, pH 7.0) was added to control cells. Cells were incubated at 37 °C for 1.0–1.5 h with constant rocking. After the incubation, cells were washed in HSB, strained through nylon mesh to remove aggregates, and resuspended in HSB at  $10^8$  cells/mL.

**Reagents.** Catalase, bovine serum albumin (BSA), dimethyl sulfoxide (DMSO), parahydroxyphenylacetic acid (PHPA), superoxide dismutase (SOD), horseradish peroxidase (HRP), cytochrome C, lysophosphatidylcholine, and CHO-MLF were from Sigma Chemical Co. (St. Louis, MO).  $LTB_4$  was from Biomol (Plymouth Meeting, PA). IL-8 was from R&D Systems (Minneapolis, MN). Dihydrorhodamine-123 (DHR-123) and NBD-phalloidin were from Molecular Probes (Eugene, OR). All chemoattractant ligands were dissolved in DMSO and stored in aliquots at  $-20$  °C. Prior to use the chemoattractants were diluted to <0.1% DMSO in HSB plus 1 mg/mL BSA.

**Oxidant Production Assays.** Oxidant production was measured in two ways: with a spectrofluorometric assay that gives the average response of a population of cells, and with a flow cytometric assay that gives single cell information. Before each assay was run, cells were allowed to equilibrate in HSB plus 1.5 mM  $Ca^{2+}$  for 10 min at 37 °C.

The spectrofluorometric assay was based on the protocol of Hyslop and Sklar (24). Cells at  $2 \times 10^6$ /mL were

stimulated in the presence of 167  $\mu\text{g/mL}$  PHPA, 53  $\mu\text{g/mL}$  SOD, and 53  $\mu\text{g/mL}$  HRP. Superoxide dismutase rapidly converts  $\text{O}_2^-$  to  $\text{H}_2\text{O}_2$ , which in the presence of peroxidase converts PHPA to a fluorescent diadduct. Fluorescence was monitored on an SLM 8100 spectrofluorometer with an excitation wavelength of 323 nm and an emission wavelength of 400 nm. On each experimental day a standard curve of fluorescence vs  $\text{H}_2\text{O}_2$  concentration was prepared by adding micromolar amounts of  $\text{H}_2\text{O}_2$  to the cocktail of PHPA, SOD, and HRP.

The flow cytometric assay for oxidant production was based on the protocol of Lund-Johansen and Olweus (25), and used DHR-123 as an indicator of oxidant production. Nonfluorescent DHR-123 can freely cross the cell membrane, and is irreversibly converted to fluorescent rhodamine-123 in the presence of oxidants. Rhodamine-123 is a positively charged compound and therefore becomes trapped inside of the cells, preventing leakage (26). One minute before placing cells at  $10^6/\text{mL}$  on the flow cytometer (FACScan, Becton-Dickinson, Mountain View, CA), 500 units/mL catalase and 30  $\mu\text{M}$  DHR-123 were added with immediate mixing. Catalase was necessary to minimize the diffusion of oxidants from responding to nonresponding cells. The cells were placed on the flow cytometer and 3000–10000 events were collected in order to get the mean fluorescent channel number of unstimulated (nonresponding) cells. The cells were then removed from the flow cytometer, and 100 nM CHO-MLF in HSB/BSA was added (or HSB/BSA alone to controls). Fifteen minutes after stimulus addition, the cells were placed back on the flow cytometer, and 3000–10000 events were collected to get the mean fluorescent channel number of responding cells and the percentages of responding and nonresponding cells. Before determining flow cytometric statistics, neutrophils were gated from other cells and debris based on forward and side scatter parameters. In experiments in which oxidant production and actin polymerization were to be measured pseudo-simultaneously, 90  $\mu\text{L}$  aliquots of cells were removed 1 min before and 10 s after stimulus addition and fixed in 3.7% formalin for the NBD-phalloidin F-actin assay (see below).

**Actin Polymerization Assay.** F-actin content was determined according to the method of Howard and Meyer (27). Before each assay was run, cells were allowed to equilibrate in HSB plus 1.5 mM  $\text{Ca}^{2+}$  for 10 min at 37 °C. An aliquot of cells was fixed in 3.7% formalin before and 10 s after stimulus addition. These fixed cells were permeabilized with lysophosphatidylcholine, and the F-actin was stained with NBD-phalloidin. Fluorescence was then quantified with the flow cytometer. In some experiments, F-actin content was measured pseudo-simultaneously with oxidant production.

**Setting Population Markers in FACScan Assays.** To determine the percent of cells that were responding or nonresponding in both the NBD-phalloidin F-actin assay and the DHR-123 oxidant assay, the software package Cell Quest (Becton-Dickinson) was used to set markers that defined the two populations on the fluorescence histograms. The number of cells, the percent of total cells, and the mean fluorescence channel number of the cells in each marker region were then computed. The same markers for the responding and nonresponding regions were used for all runs on the same day with neutrophils from the same donor. While the use of markers can be limited by significantly overlapping

populations, our data had sufficient separation between the two populations to give reliable results using this method.

## RESULTS

**Oxidant Production and Actin Polymerization Show Threshold Behavior in Terms of G-Protein Number.** Figure 2A shows fluorescence histograms from the NBD-phalloidin F-actin assay for maximally stimulated (100 nM  $\text{LTB}_4$ ) neutrophils which have undergone various levels of PT treatment. There is only one population of cells present in the histograms for stimulated cells that have not undergone PT treatment and for unstimulated cells. The mean channel number of the histogram for unstimulated cells gives the level of response for nonresponding (NR) cells. The mean channel number of the histogram for stimulated cells that have not undergone PT treatment gives the level of response for fully responding (R) cells. Stimulation of PT treated neutrophils resulted in two distinct populations of cells; a nonresponding population with a mean fluorescence channel number approximately equal to that of unstimulated cells, and a responding population with a higher mean fluorescence channel number approximately equal to that of stimulated, non-PT treated cells. As the number of receptor-coupled G-proteins was decreased by increasing PT treatment, the percentage of cells in the nonresponding population increased, while the level of response of the responding population of cells remained near the maximal level. This is indicative of threshold behavior and is in agreement with the data of Omann et al. (1, 2) for the CHO-MLF stimulated actin polymerization response. The cells in Figure 2A were stimulated with  $\text{LTB}_4$ , but the same behavior was observed when actin polymerization was stimulated with CHO-MLF and IL-8 (data not shown).

Fluorescence histograms from the DHR-123 oxidant production assay for CHO-MLF stimulated neutrophils are shown in Figure 2B. As with the actin polymerization response, increased PT treatment resulted in an increase in the number of nonresponding cells, while the responding population of cells had a level of response near the maximum. This responder/nonresponder behavior is consistent with the data of Lund-Johansen and Olweus (25) for CHO-MLF/cytochalasin B stimulated oxidant production, although cytochalasin B was not used in our studies.

To pool data from multiple experiments with different blood donors, the response was normalized to control cells as described in the caption to Figure 3 and plotted versus the percent of cells responding. Figure 3 shows the normalized response versus the percent of cells responding for actin polymerization stimulated by the three different chemoattractants CHO-MLF,  $\text{LTB}_4$ , and IL-8. As the percent of cells responding decreases, the normalized response remains at about 100%, as would be expected for threshold behavior. The same behavior is observed for all three chemoattractants tested.

Figure 4 shows the normalized response versus the percent of cells responding for CHO-MLF stimulated oxidant production. In this case there is some decrease in the normalized response as the percent of cells responding decreases. However, even when very few cells respond, the normalized response is still above 50% of the maximum. The dominant feature of the data is therefore threshold



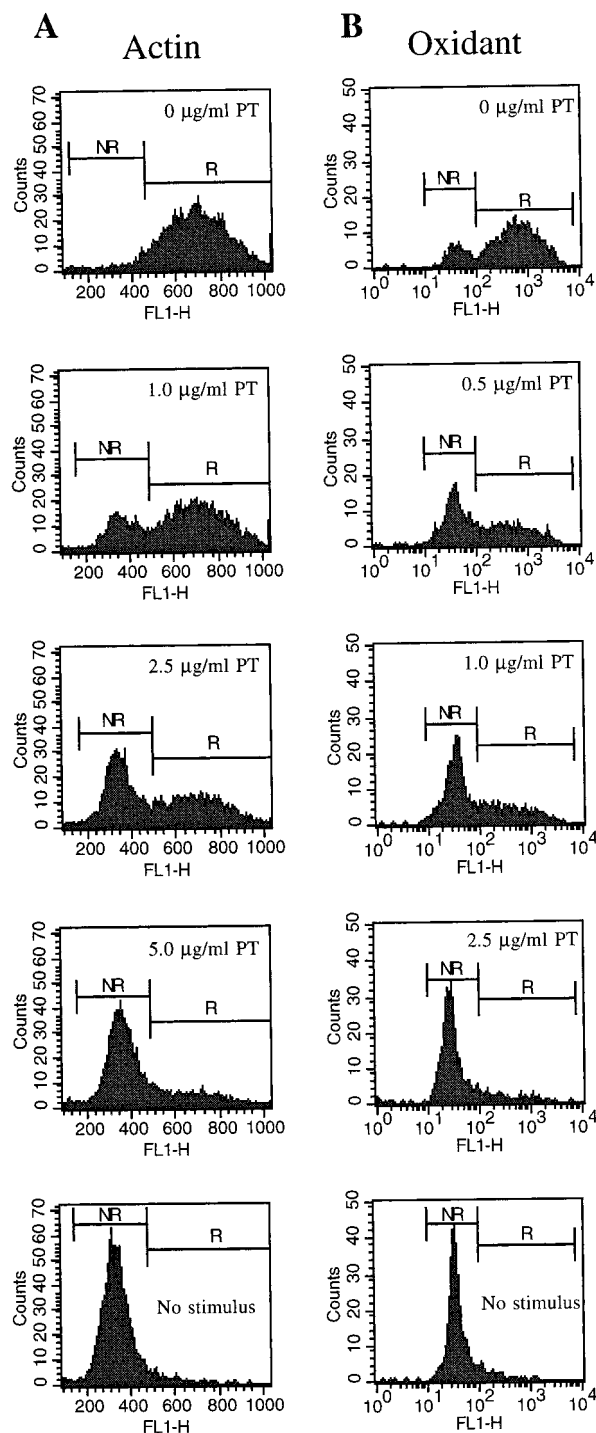


FIGURE 2: Dependence of responses on G-protein level. (A) Fluorescence histograms for the NBD-phalloidin F-actin assay when cells at the designated level of PT treatment were stimulated with 100 nM LTB<sub>4</sub>. (B) Fluorescence histograms for the DHR-123 oxidant assay when cells at the designated level of PT treatment were stimulated with 100 nM CHO-MLF. NR is the marker set for the nonresponding population of cells, and R is the marker set for the responding population of cells. Neutrophils were gated from contaminating cells based on forward and side scatter parameters before making histograms.

behavior. Decreases in mean channel number at lower percents of cells responding may be partially explained by inhibition of *N*-formyl peptide receptor upregulation caused by PT treatment. Hoffman et al. (18) recently reported that PT treatment does not affect the kinetics of *N*-formyl peptide binding to neutrophil *N*-formyl peptide receptors, but the

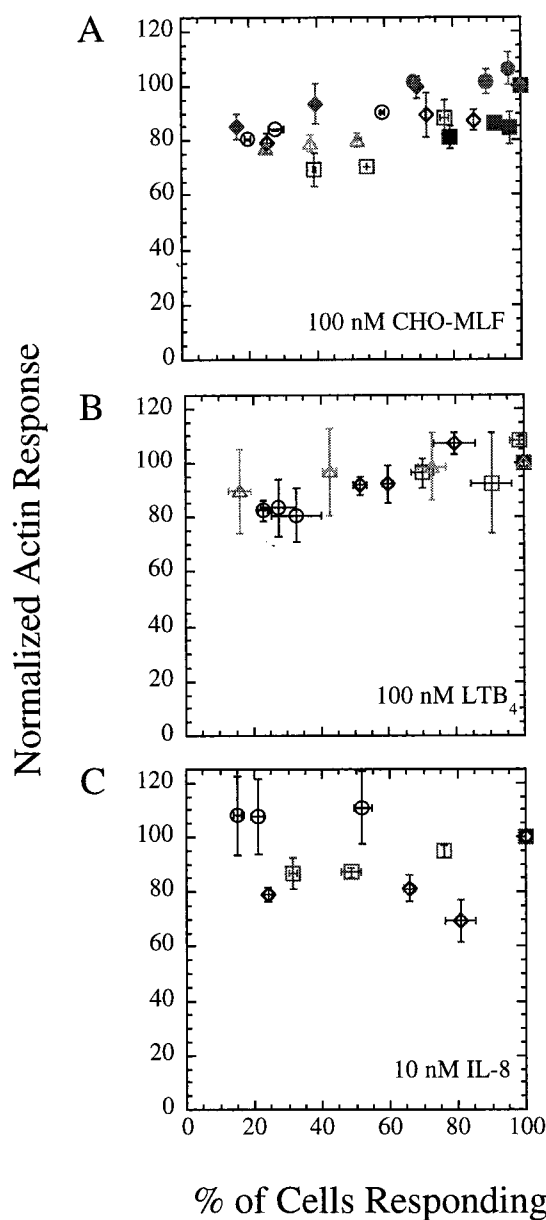


FIGURE 3: Normalized response (i.e., mean fluorescence channel number) of responding cells vs the percent of cells responding for the NBD-phalloidin F-actin assay. Each point is the average of duplicates. Different symbols represent different experiments. The percent of cells responding is normalized such that 100% corresponds to the percent of cells responding in control cells (incubated with no PT). The normalized response is calculated as  $(F_R - F_{NR})_{PT} / (F_R - F_{NR})_{Control}$ , where  $F_R$  and  $F_{NR}$  are the mean fluorescence channel numbers of the responding and nonresponding populations, respectively. Cells were stimulated with 100 nM CHO-MLF (A), 100 nM LTB<sub>4</sub> (B), or 10 nM IL-8 (C).

extent of binding is reduced by as much as 55%. This reduction in the extent of binding was attributed to inhibition of receptor upregulation. Because actin polymerization is known to require 100-fold fewer bound receptors than oxidant production (15), inhibition of receptor upregulation should not have as significant an effect on the actin polymerization response.

As a check on the DHR-123 oxidant assay, the PHPA assay of Hyslop and Sklar (24) was used to measure oxidant production, and the results were compared to those of the DHR-123 assay. The PHPA assay measures the response of a population of cells in solution. Therefore, the measured

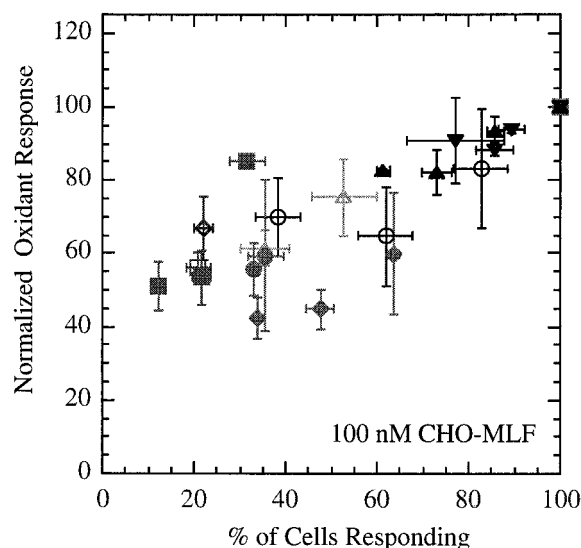


FIGURE 4: Normalized response of responding cells vs the percent of cells responding for the DHR-123 oxidant assay. Each point is the average of duplicates. Different symbols represent different experiments. The response is normalized as in Figure 3. Cells were stimulated with 100 nM CHO-MLF.

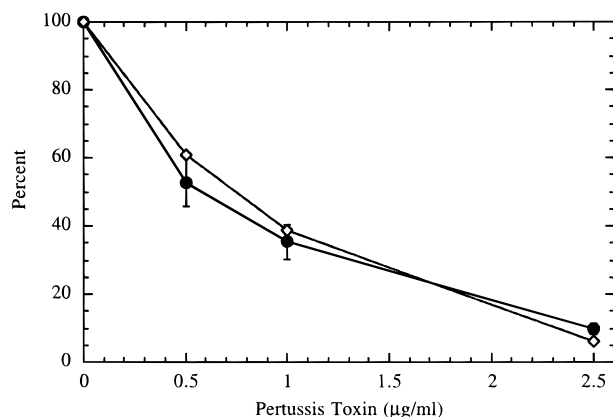


FIGURE 5: Comparison of percent of cells responding from DHR-123 single-cell oxidant assay (●) and percent control fluorescence from PHPA population average oxidant assay (◇) after incubation with various concentrations of PT. The percent of cells responding was normalized to controls as in Figure 3. The data are representative of experiments performed with neutrophils from seven donors. Each point is the average of duplicates. Cells were stimulated with 100 nM CHO-MLF.

fluorescence in this assay is the average of responding and nonresponding cells. The percent of cells responding measured in the single-cell DHR-123 oxidant assay correlates well with the percent of control fluorescence measured in the PHPA oxidant assay (Figure 5). This indicates that the decrease in fluorescence seen in the PHPA assay with increasing PT treatment is primarily due to a decrease in the number of cells responding, and not due to a decrease in the extent of response of individual cells.

An interesting point to consider is whether pertussis toxin has access to different pools of G-proteins. It is possible that there are pools of G-proteins associated with particular receptors or effectors, and these pools may be differentially accessible to PT. However, our data for the three different chemoattractants, CHO-MLF, IL-8, and LTB<sub>4</sub>, which bind to three distinct cell surface receptors, argue against this for the case of receptor-associated pools of G-protein. Figure

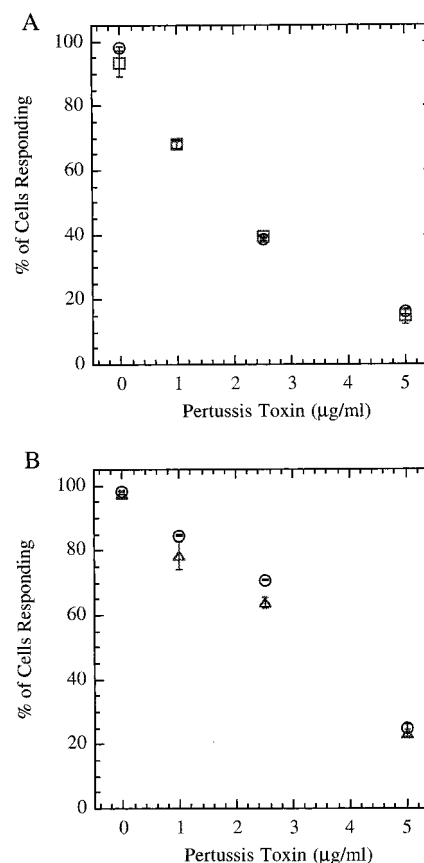


FIGURE 6: (A) Percent of cells responding in the NBD-phalloidin F-actin assay at different levels of PT treatment. Cells were stimulated with 100 nM CHO-MLF (○) or 100 nM LTB<sub>4</sub> (□). Data are representative of experiments performed with neutrophils from four donors and are the average of duplicates run on the same day. (B) Same as in A except cells were stimulated with 100 nM CHO-MLF (○) or 10 nM IL-8 (△). Data are representative of experiments performed with neutrophils from three donors and are the average of duplicates run on the same day.

6 shows the percent of cells responding in the actin polymerization assay at different levels of PT treatment for cells stimulated with CHO-MLF or LTB<sub>4</sub> (A) and CHO-MLF or IL-8 (B). In both cases, PT affects the percent of cells responding to IL-8 or LTB<sub>4</sub> stimulation to the same extent that it affects the percent of cells responding to CHO-MLF stimulation. It therefore appears that either G<sub>i</sub>-proteins in neutrophils are not segregated into pools associated with different chemoattractant receptors, or PT has equal access to all of these pools.

**Differential Sensitivity of Actin Polymerization and Oxidant Production.** Oxidant production and actin polymerization were assayed pseudo-simultaneously on the single-cell level after neutrophils were incubated with various concentrations of PT. As shown in Figure 7, oxidant production was considerably more sensitive to PT treatment than actin polymerization. In a representative experiment, incubation of cells with 2.5 μg/mL PT for 1.5 h resulted in a 90% inhibition of oxidant production, but only a 40% inhibition of actin polymerization. This is in agreement with the previously reported data of Omann et al. (2) in which the cell population PHPA assay was used to measure oxidant production. Since we have now used a single-cell assay to show that oxidant production exhibits threshold behavior in terms of G-protein number, the fact that a given level of PT

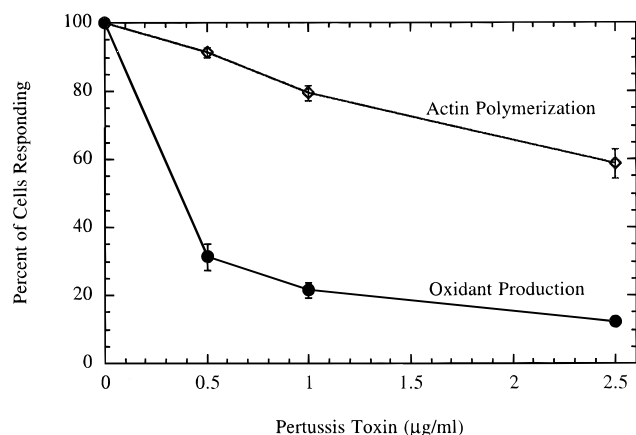


FIGURE 7: Comparison of the percent of cells responding as measured in the DHR-123 oxidant assay (●) and the NBD-phalloidin F-actin assay (◇) after incubation with various concentrations of PT. The two responses were measured pseudo-simultaneously, and the percent of cells responding was normalized to control cells incubated with no PT. Data are representative of experiments performed with neutrophils from two donors. Each point is the average of duplicates. The cells were stimulated with 100 nM CHO-MLF.

treatment resulted in a significantly larger decrease in the percent of cells responding for oxidant production than for actin polymerization suggests that the threshold number of G-proteins required for the two responses is different. Evidently a larger number of coupled G-proteins is required for oxidant production.

**Graded Ligand Stimulation Results in Different Behavior Than Graded G-Protein Uncoupling.** When neutrophils were stimulated with submaximal doses of ligand, the resulting responses showed distinctly different behavior than when the cells were treated with varying concentrations of PT prior to stimulation. Figure 8A shows the fluorescence histograms for the actin polymerization response stimulated with various concentrations of CHO-MLF. As was seen by Omann et al. (2), only a single population of cells was present in these histograms, and as the ligand concentration was decreased the entire population shifted to a lower level of response. This is indicative of graded behavior which is characterized by a hyperbolic dose-response curve, and is in sharp contrast to the threshold behavior seen with graded G-protein uncoupling. The same behavior was seen when actin polymerization was stimulated with LTB<sub>4</sub> and IL-8 (data not shown).

Figure 8B shows fluorescence histograms for the oxidant production response stimulated with various concentrations of CHO-MLF. In this case there are two populations of cells observed. However, as the concentration of CHO-MLF is decreased the responding population of cells shifts to a lower level of response. This decrease in the level of response is more significant than when the cells were PT treated prior to stimulation with ligand (Figures 2, 4). Figure 9 shows the percent of cells responding versus the normalized oxidant production response for cells stimulated with various concentrations of CHO-MLF. As the data in Figure 9 approaches zero percent of cells responding, the normalized response approaches zero percent, whereas in Figure 4 the normalized response is still ~50%. Oxidant production appears to show a combination of graded and threshold behavior, with graded behavior dominating as the ligand

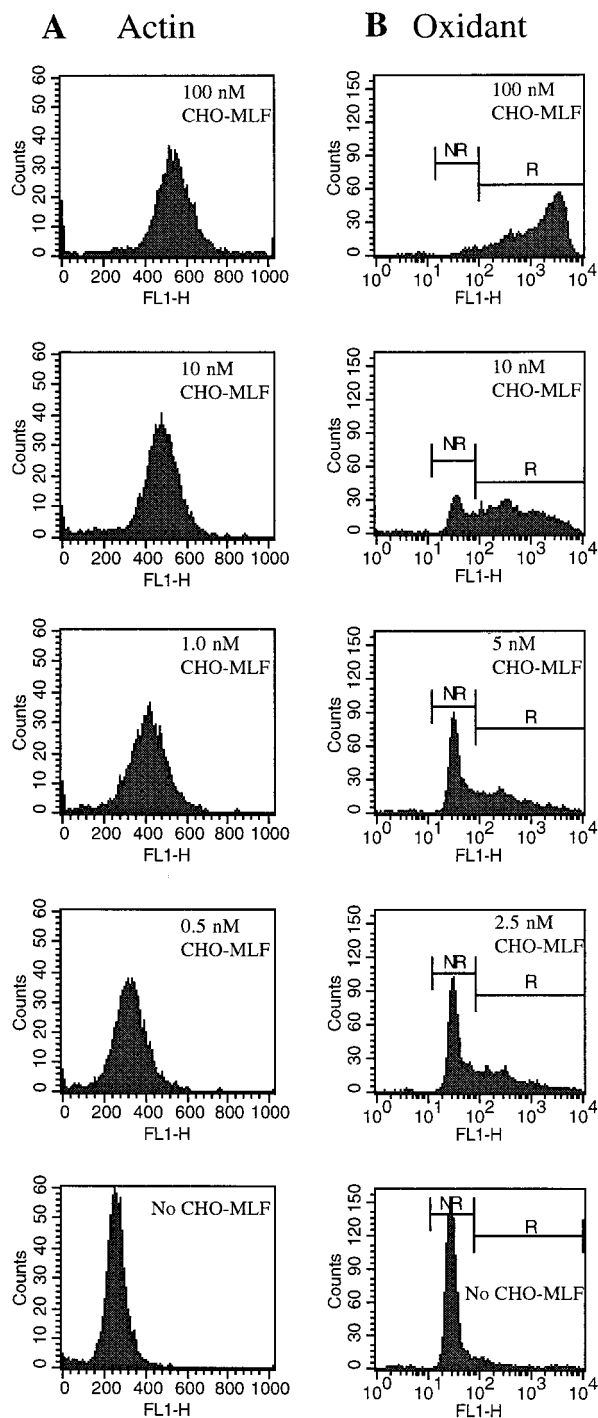


FIGURE 8: Dependence of responses on ligand concentration. (A) Fluorescence histograms for the NBD-phalloidin F-actin assay when cells were stimulated with CHO-MLF at the designated concentrations. (B) Fluorescence histograms for the DHR-123 oxidant assay when cells were stimulated with CHO-MLF at the designated concentrations. NR is the marker set for the non-responding population of cells, and R is the marker set for the responding population of cells. Neutrophils were gated from contaminating cells based on forward and side scatter parameters before making histograms.

concentration is varied, and threshold behavior dominating as the G-protein number is varied.

**Trends in Experimental Data Can Be Elucidated with a Simple Mathematical Model.** To explain the different behaviors observed for actin polymerization and oxidant production when neutrophils undergo graded G-protein

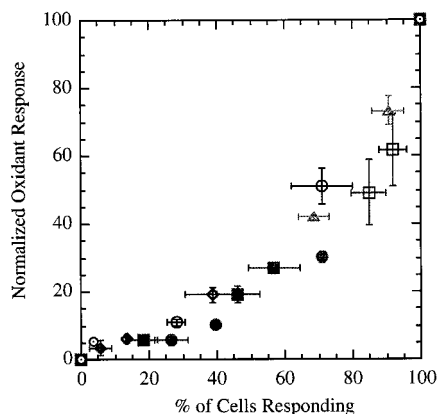


FIGURE 9: Normalized response of responding cells vs the percent of cells responding for the DHR-123 oxidant assay as ligand concentration is varied. Each point is the average of duplicates. Different symbols represent different experiments. To correct for unstimulated cells which may have fallen in the region marked as the responding population, the level of response and % of cells responding were normalized using the following equations: normalized response =  $[(F_R)(R) - (F_{R,unstim})(R_{unstim})] / [(F_{R,max})(R_{max}) - (F_{R,unstim})(R_{unstim})] \times 100$  and % of cells responding =  $[(R - R_{unstim}) / (R_{tot} - R_{unstim})] / [(R_{max} - R_{unstim}) / (R_{tot,max} - R_{unstim})] \times 100$  where  $F_R$  is the mean channel number of responding cells,  $R$  is the number of responding cells,  $F_{R,unstim}$  is the mean channel number of cells that fall within the responding marker in unstimulated samples,  $R_{unstim}$  is the number of cells that fall within the responding marker in unstimulated samples,  $F_{R,max}$  is the mean channel number of responding cells stimulated with 100 nM CHO-MLF,  $R_{max}$  is the number of cells responding upon stimulation with 100 nM CHO-MLF,  $R_{tot}$  is the total number of cells, and  $R_{tot,max}$  is the total number of cells in samples stimulated with 100 nM CHO-MLF. This normalization procedure gives a normalized response of 100 for cells stimulated with 100 nM CHO-MLF and zero for unstimulated cells.

uncoupling as compared to graded ligand stimulation, we postulated a simple mathematical model. Varying either the number of G-proteins or the ligand concentration is expected to change the amount of G-protein that is activated upon stimulation. If the ensuing responses were controlled directly by the amount of activated G-protein, one would expect that varying G-protein and ligand concentration would result in the same type of response behavior (see Appendix for details). However, our experiments showed quite different response behavior depending on whether G-protein number or ligand concentration was varied, and the behavior was different for actin polymerization and oxidant production. This suggests that the responses cannot simply be a function of the number of activated G-proteins. We therefore hypothesized an additional G-protein independent functionality, and expressed the response as

$$\text{Response} = f_1(G,L) f_2(L) \quad (1)$$

The function  $f_1$  depends on G-protein number and ligand concentration through the number of activated G-proteins ( $G^*$ ) and was made to be a steep threshold function by using a Michaelis–Menten type expression with a Hill coefficient ( $n$ ) greater than 1:

$$f_1 = \left( \frac{[G^*]^n}{K_{m1}^n + [G^*]^n} \right) \quad (2)$$

$G^*$  may either be the  $\alpha$  subunit or the  $\beta\gamma$  subunits of the G-protein. Hill coefficients greater than 1 have been reported

for the mitogen-activated protein kinase cascade, and are thought to result from having a number of enzymes which follow Michaelis–Menten type kinetics in series (7, 8). Because this function is very steep,  $K_{m1}$  simply represents the threshold number of activated G-proteins necessary for a response to occur. Since oxidant production was shown to have a higher threshold for G-protein than actin polymerization (Figure 5), we modeled the two responses by making the value of  $K_{m1}$  higher for oxidant production than for actin polymerization.

The function  $f_2$  depends on the ligand concentration through the number of low-affinity ligand/receptor complexes ( $LR_s$ ) and was made to be a graded function by using a Michaelis–Menten type expression with the Hill coefficient equal to one:

$$f_2 = \left( \frac{[LR_s]}{K_{m2} + [LR_s]} \right) \quad (3)$$

Although  $f_2$  is expressed here as a function of  $LR_s$ , it may in reality depend on a downstream event other than G-protein activation that is triggered by ligand/receptor complexes. Also note that both  $f_1$  and  $f_2$  are required for a response to occur in this model.

The values for  $G^*$  and  $LR_s$  used in the functions  $f_1$  and  $f_2$  are the integrated values over the time that the model was run. The model was typically run for a total time of 240 s because both actin polymerization and oxidant production are known to be completed within 4 min. To get the integrated values, we needed to include ligand/receptor binding and G-protein activation reactions in the model. The ligand/receptor binding model used was developed by Hoffman et al. (18, 19), and the values of the rate constants used were based on those measured by Hoffman et al. (18) for the *N*-formyl peptide CHO-NLFNTK-fl at 37 °C (details and values are given in the appendix). The model involves conversion of the ligand/receptor complex from a low-affinity ( $LR_s$ ) to a high-affinity ( $LR_h$ ) form. To account for the cell-to-cell heterogeneity which is observed experimentally, individual cell parameters (i.e., receptor number, G-protein number, and rate constants) were chosen randomly from a normal distribution with a given mean and standard deviation and the model was run 1000 times to simulate a population of cells.

Figure 10 shows model results for the actin polymerization (A) and oxidant production (B) responses when the total number of G-proteins was varied. As the number of G-proteins was decreased, the number of cells exhibiting actin polymerization decreased, indicating that some cells could no longer reach the threshold for  $G^*$ . Using the same number of G-proteins as in the simulations in Figure 10A, the number of cells undergoing oxidant production decreased much more rapidly as G-protein number was decreased. As expected, different  $G^*$  thresholds for actin polymerization and oxidant production were achieved when the value of  $K_{m1}$  for the two responses was different.

Figure 11 shows model results for actin polymerization (A) and oxidant production (B) as the ligand concentration was decreased. For actin polymerization, as the ligand concentration was decreased there was only one population of cells which shifted to a lower level of response. For oxidant production, as ligand concentration was decreased



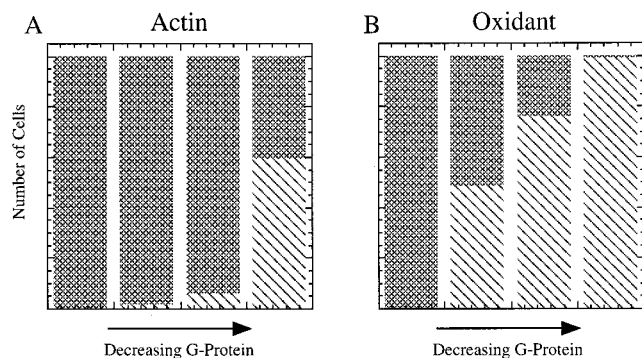


FIGURE 10: Model predictions for actin polymerization (A) and oxidant production (B) as the number of G-proteins is varied. The percent of cells responding is plotted as a function of the G-protein number. Responding cells exhibited maximal or nearly maximal levels of response. Model parameters are given in Table 1 in the Appendix. Stippled area: responding cells. Area with diagonal lines: nonresponding cells.

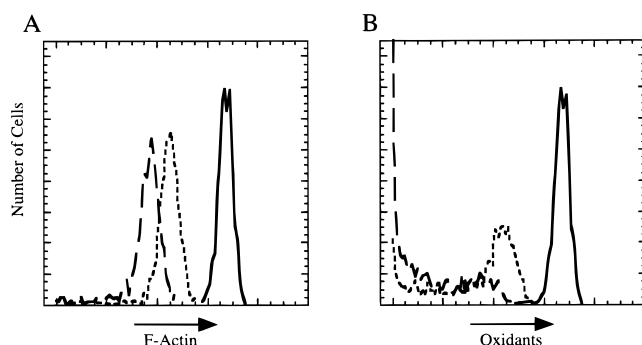


FIGURE 11: Model predictions for actin polymerization (A) and oxidant production (B) as the ligand concentration is varied (0.5 nM —; 0.13 nM - - -; 0.09 nM —). As the ligand concentration decreases, the cellular response also decreases. Binding kinetics were based on reported values for CHO-NLFTK-fl, and model parameters are given in Table 1 in the appendix.

the cells shifted to a lower level of response, but in addition a second and nonresponding population of cells appeared (see curve for 5 nM). The model results for varying G-protein number and ligand concentration are therefore qualitatively consistent with our experimental data.

## DISCUSSION

Using single-cell flow cytometric assays in conjunction with PT treatment of human neutrophils, we have shown that a threshold number of receptor-coupled G-proteins is required to transduce the signals leading to both actin polymerization and oxidant production. As the number of receptor-coupled G-proteins is decreased through increased PT treatment, the number of nonresponding cells increases, while the responding cells continue to respond at or near a maximal level. For the actin polymerization response we have shown that this threshold behavior exists for three different chemoattractants which bind to three different receptors. In addition, our data for these three different receptors suggests that either G-proteins are not segregated into receptor-associated pools or that PT has equal access to all of these pools of G-proteins. This is consistent with work by Jacobs et al. (28) which concludes that there are not receptor-associated pools of G-proteins based on ligand-mediated changes in binding of GTP $\gamma$ S to cell membranes.

For the *N*-formyl peptide receptor, we have shown that threshold behavior is observed for two different responses. In addition, threshold behavior has also been shown for CHO-MLF stimulated intracellular Ca<sup>2+</sup> elevation (2, 3). Thus threshold behavior in terms of G-protein number appears to be a general phenomena for neutrophil responses stimulated by chemoattractants. Oxidant production was found to be more sensitive to PT treatment than actin polymerization, indicating that the threshold number of receptor coupled G-proteins required for oxidant production is greater. This makes sense physiologically since the negative effects of over-stimulating actin polymerization are not nearly as detrimental as over-stimulation of oxidant production, which can lead to severe damage of host tissue (9–11).

When neutrophils were stimulated with various concentrations of ligand we saw a distinctly different behavior than was observed when the extent of PT treatment was varied. For the actin polymerization response, only one population of cells was observed at submaximal ligand concentrations. As the ligand concentration was decreased, the entire population shifted to a lower level of response. For the oxidant production response two populations of cells were observed at submaximal ligand concentrations. However, as ligand concentration was decreased the level of response decreased. Oxidant production appears to show a combination of graded and threshold behavior in terms of both G-protein and ligand with threshold behavior playing a larger role as G-protein is decreased and graded behavior playing a larger role as ligand concentration is decreased.

It could be hypothesized that the differential effect of PT on the actin polymerization and oxidant production responses was due to differential access of the PT to effector-associated pools of G-proteins. Since Ca<sup>2+</sup> elevation and oxidant production are both consequences of G-protein activation of phospholipase C (i.e., the G-protein effector), this hypothesis would predict that the Ca<sup>2+</sup> and oxidant responses would have the same threshold for activated G-proteins. The observation that this is not the case (1–3) argues against there being effector-associated pools of G-proteins that are differentially affected by PT. Moreover, this cannot explain the different characteristics of the response behavior for actin polymerization (graded) and oxidant production (graded and threshold) with varying ligand concentration.

To explain the differences in response behavior observed when G-protein and ligand concentration were varied, we developed a simple mathematical model for actin polymerization and oxidant production. The different behaviors cannot be accounted for by simply having all of the signal transduction events following G-protein activation directly controlled by the number of activated G-proteins (see Appendix). To get both the observed graded and threshold behavior, something in addition to, and not initiated by, G-protein must be contributing to the response. In our model we made the response proportional to two functions:  $f_1$ , a steep threshold function dependent on activated G-protein, and  $f_2$ , a graded function dependent on the number of low-affinity ligand/receptor complexes or a downstream signal other than G-protein activation initiated by these complexes. The threshold behavior of the responses is controlled by  $f_1$ , while the graded behavior is controlled by  $f_2$ . The math-



ematical model gives results qualitatively consistent with our experimental observations.

In the model, the overall behavior of the response is determined by the value of the threshold  $K_{m1}$  relative to the integrated value of  $G^*$  over the particular range of ligand concentrations or G-protein numbers chosen. For the actin polymerization response, as ligand concentration is decreased the model gives only one population of cells, and this population shifts to a lower level of response. This is achieved by setting  $K_{m1}$  low enough so that  $G^*$  only falls below the threshold at very low ligand concentrations. The main character of the response is then given by eq 3 which is graded in terms of ligand concentration. As the number of G-proteins is decreased in the model, threshold behavior results for actin polymerization. Since changing the number of G-proteins only effects  $G^*$ , the character of the response is controlled by eq 2, a threshold function. For oxidant production, as ligand concentration is decreased, we see a combination of graded and threshold behavior. This is because  $K_{m1}$  is set to a value high enough that as ligand concentration is decreased  $G^*$  falls below the threshold, resulting in a nonresponding population. The character of the response is governed by both eqs 2 and 3. As the number of G-proteins is decreased, threshold behavior is observed since the response is controlled by eq 2.

Our work has implications for understanding a variety of responses initiated by G-protein coupled receptors. Rather than just assuming that the response is proportional to the amount of activated G-protein (e.g., refs 29–31), other early signal transduction events that are not initiated by G-protein activation need elucidation. In the neutrophil, there are several possibilities for these early events that could influence response behavior. The conversion of neutrophil *N*-formyl peptide ligand/receptor complexes from a low-affinity to a high-affinity form has been shown to be G-protein independent (17–19). This conversion affects the number of ligand/receptor complexes in a particular state, and thus influences the function  $f_2$  in our model and contributes to the response characteristics. Another G-protein independent event which may influence signal transduction is the association of ligand/receptor complexes with the cytoskeleton (20–22). Our experimental and theoretical work suggests the novel hypothesis that one or more of these pathways is important for controlling or modulating neutrophil responses.

## APPENDIX

The description of ligand/receptor binding kinetics used in our model is based on the work of Hoffman et al. (18, 19) and Sklar (32) for the *N*-formyl peptide receptor of human neutrophils. Hoffman et al. (18) included ligand association and dissociation, receptor upregulation, ligand/receptor complex internalization, and the conversion of the receptor from a low-affinity form ( $LR_s$ ) to a high-affinity form ( $LR_x$ ). A schematic of their model with the step of G-protein activation added is shown in Figure 12. The steps of ligand dissociation and rebinding to  $LR_x$  and internalization of  $LR_x$  were omitted from the Hoffman et al. model as they do not play a role in generating the G-protein activation we aimed to describe here. The model in Figure 12 is described by the following differential equations:

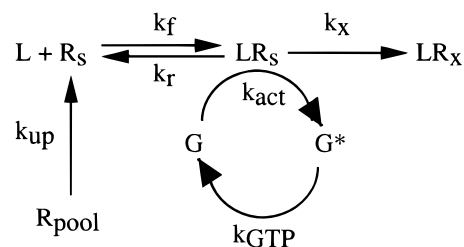


FIGURE 12: Schematic of ligand binding and G-protein activation. L is ligand,  $R_s$  is the signaling form of the receptor,  $LR_s$  is the signaling ligand/receptor complex,  $LR_x$  is the nonsignaling ligand/receptor complex,  $R_{pool}$  is an intracellular pool of receptors which is upregulated, G is G-protein, and  $G^*$  is activated G-protein. Rate constants are defined in Table 1.

Table 1. Parameters Used in the Mathematical Model<sup>a</sup>

parameter	definition	mean value
$k_f$	ligand association rate constant for $R_s$	$8.4 \times 10^7 \text{ M}^{-1} \text{ s}^{-1}$
$k_r$	ligand dissociation rate constant for $R_s$	$0.37 \text{ s}^{-1}$
$k_x$	rate constant for conversion of $R_s$ to $R_x$	$6.5 \times 10^{-2} \text{ s}^{-1}$
$k_{up}$	rate constant for upregulation of $R_s$	$8.0 \times 10^{-4} \text{ s}^{-1}$
$k_{act}$	activation rate constant for G to $G^*$	$1.0 \times 10^{-7} \text{ s}^{-1}$
$k_{GTP}$	inactivation rate constant for $G^*$	$2.0 \times 10^{-1} \text{ s}^{-1}$
$R_s(t=0)$	total initial number of surface receptors	$5.5 \times 10^4$
$R_{pool}(t=0)$	initial pool of receptors that can be upregulated	$2.5 \times 10^4$
$G_{tot}$	total number of G-proteins	$5 \times 10^3 - 1 \times 10^5$

<sup>a</sup> Note that all values are mean values.

$$d[L]/dt = (k_r[LR_s] - k_f[L][R_s])(N/(Av)) \quad (A1)$$

$$d[R_s]/dt = k_r[LR_s] - k_f[L][R_s] + k_{up}[R_{pool}] \quad (A2)$$

$$d[LR_s]/dt = k_f[L][R_s] - k_r[LR_s] - k_x[LR_s] \quad (A3)$$

$$d[LR_x]/dt = k_x[LR_s] \quad (A4)$$

$$d[R_{pool}]/dt = -k_{up}[R_{pool}] \quad (A5)$$

$$d[G^*]/dt = k_{act}[LR_s][G] - k_{GTP}[G^*] \quad (A6)$$

$$d[G]/dt = k_{GTP}[G^*] - k_{act}[LR_s][G] \quad (A7)$$

where  $Av$  is Avogadro's number and  $N$  is the cell concentration per volume.

These differential equations were solved numerically using the parameters listed in Table 1. The values for the parameters used in each run of the model were chosen randomly from a normal distribution with the mean set to the value in Table 1, and a standard deviation equal to 10% of the mean (20% for G-protein number). The model was run 1000 times to simulate a population of cells. The response of each cell (i.e., each run of the model) was calculated using the integrated values of  $G^*$  and  $LR_s$  over the time that the model was run in the following equation:

$$\text{Response} = V_m \left( \frac{[G^*]^n}{K_{m1}^n + [G^*]^n} \right) \left( \frac{[LR_s]}{K_{m2} + [LR_s]} \right) \quad (A8)$$

where  $V_m$ , the maximum value of the response, was set to 100,  $n$  was set to 10,  $K_{m2}$  was set to  $3 \times 10^5$ , and  $K_{m1}$  was set to  $5 \times 10^3$  for modeling actin polymerization and  $1 \times 10^4$  for modeling oxidant production. The model was run

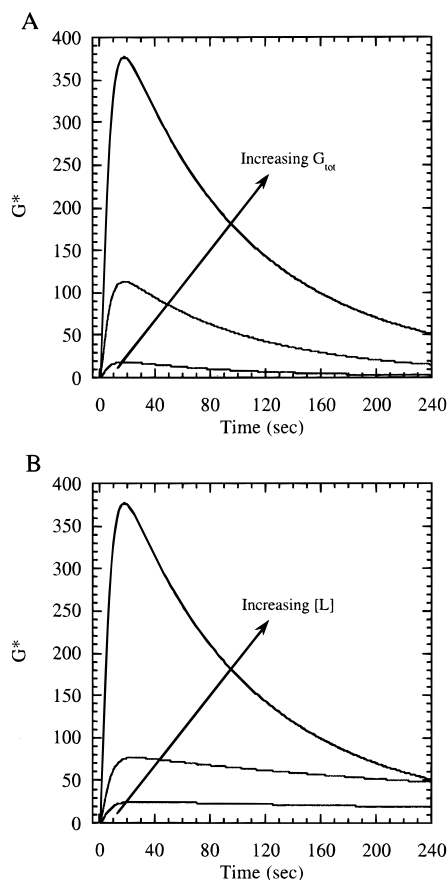


FIGURE 13: (A) Effect of varying the total G-protein number on the amount of activated G-protein ( $G^*$ ) produced. (B) Effect of varying the ligand concentration on the amount of  $G^*$  produced. Varying either the total number of G-proteins or the ligand concentration has a similar effect on the amount of  $G^*$  produced, suggesting that if the response depended only on  $G^*$  similar response behavior would be observed. However, different response behavior is seen experimentally (see Figures 2, 3, 4, 8, and 9)

for a total time of 240 s. This time was chosen because both actin polymerization and oxidant production are known to be completed within 4 min.

The function in eq A8 was used to model responses because different response behavior was observed experimentally depending on whether G-protein number or ligand concentration was varied, and the response behavior was different for actin polymerization and oxidant production. If the responses were made only a function of activated G-protein ( $G^*$ ), these differences in behavior would not be produced because the net effects of varying G-protein and ligand concentration on the amount of  $G^*$  are approximately equivalent. This can be shown by using eqs A1–A7 to solve for the amount of  $G^*$  produced with different total G-protein numbers and initial ligand concentrations. Figure 13 shows the results from these simulations. These results suggest that the responses cannot simply be a function of the number of activated G-proteins, or similar behavior would be seen when either G-protein number or ligand concentration is varied.

## REFERENCES

1. Omann, G. M., Harter, J. M., Hassan, N., Mansfield, P. J., Suchard, S. J., and Neubig, R. R. (1992) *J. Immunol.* 149, 2172–2178.
2. Omann, G. M., and Porasik-Lowes, M. M. (1991) *J. Immunol.* 146, 1303–1308.
3. Omann, G. M., and Harter, J. M. (1991) *Cytometry* 12, 252–259.
4. Agrawal, N. G., and Linderman, J. J. (1995) *Biophys. J.* 69, 1178–1190.
5. Mahama, P. M., and Linderman, J. J. (1994) *Biotechnol. Prog.* 10, 45–54.
6. Mahoney, M. G., Randall, C. J., Linderman, J. J., Gross, D. J., and Slakey, L. L. (1992) *Mol. Biol. Cell* 3, 493–505.
7. Huang, C. F., and Ferrell, J. E. (1996) *Proc. Natl. Acad. Sci. U.S.A.* 93, 10078–10083.
8. Kholodenko, B. N., Hoek, J. B., Westerhoff, H. V., and Brown, G. C. (1997) *FEBS Lett.* 414, 430–444.
9. Edwards, S. E., and Hallett, M. B. (1997) *Immunol. Today* 18, 320–324.
10. Anderson, R. (1995) *S. Afr. Med. J.* 85, 1024–1028.
11. Boxer, G. J., Curnutte, J. T., and Boxer, L. A. (1985) *Hosp. Pract.*, March 15, 1985, 69–90.
12. Omann, G. M., Allen, R. A., Bokoch, G. M., Painter, R. G., Traynor, A. E., and Sklar, L. A. (1987) *Physiol. Rev.* 67, 285–315.
13. Bommakanti, R. K., Bokoch, G. M., Tolley, J. O., Schreiber, R. E., Siemsen, D. W., Klotz, K. N., and Jesaitis, A. J. (1992) *J. Biol. Chem.* 267, 7576–7581.
14. Omann, G. M. (1998) in *Phagocytic Function: A Guide for Research and Clinical Evaluation* (Robertson, J. P., and Babcock, G., Eds.) Wiley-Liss, New York (in press).
15. Sklar, L. A. (1986) *Adv. Immunol.* 39, 95–143.
16. Bokoch, G. M. (1995) *Blood* 86, 1649–1660.
17. Sklar, L. A., Bokoch, G. M., Button, D., and Smolen, J. E. (1987) *J. Biol. Chem.* 262, 135–139.
18. Hoffman, J. F., Linderman, J. J., and Omann, G. M. (1996) *J. Biol. Chem.* 271, 18394–18404.
19. Hoffman, J. F., Keil, M. L., Riccobene, T. A., Omann, G. M., and Linderman, J. J. (1996) *Biochemistry* 35, 13047–13055.
20. Jesaitis, A. J., and Klotz, K. N. (1993) *Eur. J. Haematol.* 51, 288–293.
21. Klotz, K. N., and Jesaitis, A. J. (1994) *BioEssays* 16, 193–198.
22. Klotz, K. N., Krotec, K. L., and Jesaitis, A. J. (1994) *J. Immunol.* 152, 801–810.
23. Tolley, J. O., Omann, G. M., and Jesaitis, A. J. (1987) *J. Leukocyte Biol.* 42, 43–50.
24. Hyslop, P. A., and Sklar, L. A. (1984) *Anal. Biochem.* 141, 280–286.
25. Lund-Johansen, F., and Olweus, J. (1992) *Cytometry* 13, 693–702.
26. Royal, J. A., and Ischiropoulos, H. (1993) *Arch. Biochem. Biophys.* 302, 348–355.
27. Howard, T. H., and Meyer, W. H. (1984) *J. Cell Biol.* 98, 1265–1271.
28. Jacobs, A. A., Huber, J. L., Ward, R. A., Klein, J. B., and McLeish, K. R. (1995) *J. Leukocyte Biol.* 57, 679–686.
29. Shea, L., and Linderman, J. J. (1997) *Biochem. Pharmacol.* 53, 519–530.
30. Adams, J. A., Linderman, J. J., and Omann, G. M. (1998) *J. Theor. Biol.* (in press).
31. Kenakin, T. (1996) *Pharmacol. Rev.* 48, 413–463.
32. Sklar, L. A. (1985) *Biophys. J.* 47, 165a.

BI973133E